
Enhanced conduction band density of states in intermetallic EuTSi_3 (T=Rh, Ir)

A. MAURYA¹, P. BONVILLE², A. THAMIZHAVEL¹ and S. K. DHAR¹

¹ *Department of Condensed Matter Physics and Materials Science, Tata Institute of Fundamental Research, Homi Bhabha Road, Colaba, Mumbai 400 005, India*

² *CEA, Centre d'Etudes de Saclay, DSM/IRAMIS/Service de Physique de l'Etat Condensé and CNRS UMR 3680, 91191 Gif-sur-Yvette, France*

PACS 71.27.+a – Strongly correlated electron systems

PACS 75.50.Ee – Antiferromagnetic materials

PACS 76.80.+y – Mössbauer spectroscopy

Abstract – We report on the physical properties of single crystalline EuRhSi_3 and polycrystalline EuIrSi_3 , inferred from magnetisation, electrical transport, heat capacity and ^{151}Eu Mössbauer spectroscopy. These previously known compounds crystallise in the tetragonal BaNiSn_3 -type structure. The single crystal magnetisation in EuRhSi_3 has a strongly anisotropic behaviour at 2 K with a spin-flop field of 13 T, and we present a model of these magnetic properties which allows the exchange constants to be determined. In both compounds, specific heat shows the presence of a cascade of two close transitions near 50 K, and the ^{151}Eu Mössbauer spectra demonstrate that the intermediate phase has an incommensurate amplitude modulated structure. We find anomalously large values, with respect to other members of the series, for the RKKY Néel temperature, for the spin-flop field (13 T), for the spin-wave gap ($\simeq 20\text{-}25\text{ K}$) inferred from both resistivity and specific heat data, for the spin-disorder resistivity in EuRhSi_3 ($\simeq 35\ \mu\text{Ohm.cm}$) and for the saturated hyperfine field (52 T). We show that all these quantities depend on the electronic density of states at the Fermi level, implying that the latter must be strongly enhanced in these two materials. EuIrSi_3 exhibits a giant magnetoresistance ratio, with values exceeding 600% at 2 K in a field of 14 T.

Introduction. – Divalent-Eu intermetallic compounds order magnetically due to the indirect RKKY exchange interaction [1] between the Eu 4f-spins. Several Eu-based compounds with composition EuTX_3 , where T is a *d*-transition element and X = Si or Ge, crystallizing in the non-centrosymmetric BaNiSn_3 -type structure are known. Of these, the magnetic properties of EuPtSi_3 [2], EuPtGe_3 [3], EuPdGe_3 [4] and EuNiGe_3 [5, 6] have recently been reported in the literature in single crystal samples. In these materials, an anisotropic behaviour of the 2 K magnetisation seems to be the prerequisite for the existence of a cascade of close transitions, around 15 K: a transition from the paramagnetic to an incommensurate, moment modulated antiferromagnetic (AF) state occurs first, followed by another one to a single moment regular AF state, a few K below. This is the case for EuPtSi_3 and EuNiGe_3 , whereas EuPtGe_3 shows a unique transition and an isotropic behaviour of the magnetisation.

Here, we report on the magnetic properties of isostructural EuTSi_3 (T=Rh and Ir) compounds, with a single crystal sample for EuRhSi_3 only. An early Mössbauer spectroscopy study of these two compounds was performed in Ref. [7]. We show that these two materials belong to the “transition cascade” type, with an anisotropic behaviour of the magnetisation documented for EuRhSi_3 . We present in addition specific heat, transport and ^{151}Eu Mössbauer spectroscopy data. We find that the magnetic and transport properties in these two materials are notably enhanced with respect to those in other members of the series, and we show that this enhancement can be attributed to an unusually large density of conduction electron states at the Fermi level $n(E_F)$. As a remarkable result, the values of the spin-wave gap derived from such different techniques as resistivity, specific heat and single crystal magnetisation measurements are in good agreement.

Experimental. – Polycrystalline samples of EuIrSi_3 and EuRhSi_3 were prepared by melting Eu (99.9% purity), Ir/Rh (99.99%) and Si (99.999%) in an arc furnace under an inert argon atmosphere. Single crystal growth of the two Eu compounds was tried using Sn and In as flux and following the same protocol as reported in Refs. [2, 3]. Powder-diffraction spectra were recorded on a Phillips Pan-analytical set up using $\text{Cu-K}\alpha$ radiation. The magnetisation as a function of field (up to 16 T) and temperature (1.8 to 300 K) was measured using Quantum Design MPMS and VSM magnetometers. The electrical resistivity between 1.8 and 300 K in zero and applied fields, and the heat capacity were measured in a Quantum Design PPMS set-up. ^{151}Eu Mössbauer spectra were recorded at various temperatures using a commercial $^{151}\text{SmF}_3$ source mounted on a constant acceleration spectrometer.

Results and Discussion. –

Structure. Our attempt to grow single crystals succeeded only for EuRhSi_3 , with In as flux. Powder diffraction spectra of EuIrSi_3 and EuRhSi_3 could be indexed on the basis of the BaNiSn_3 type structure (space group $I4mm$). The lattice parameters obtained by the Rietveld analysis of the powder diffraction spectra are in good agreement with the previously reported values [7].

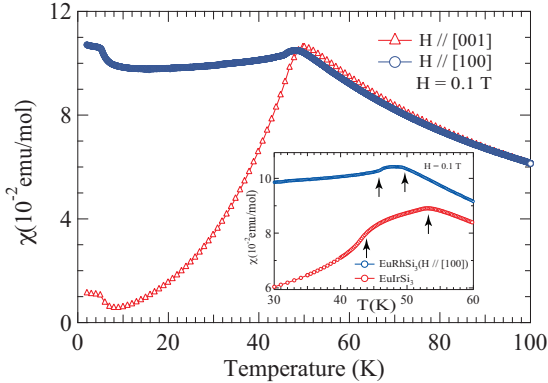


Fig. 1: Magnetic susceptibility $\chi(T)$ of single crystalline EuRhSi_3 with a field of 0.1 T along [001] and [100]. The slight increase of χ below 8 K is due to some parasitic phase, though no unidentified line appears in the x-ray diffraction spectrum. Inset: close-up of $\chi(T)$ for EuRhSi_3 with $H \parallel [100]$ and for polycrystalline EuIrSi_3 .

Susceptibility and isothermal magnetisation. The susceptibility of EuRhSi_3 measured in a field of 0.1 T applied along [001] and [100] is shown below 60 K in Fig.1. It is strongly anisotropic and a clear peak near 49 K shows the onset of the AF phase. The close-up in the inset of Fig.1 shows that this peak is split (arrows). In agreement with the heat capacity and ^{151}Eu Mössbauer data (*vide infra*), these two peaks correspond to closely spaced magnetic transitions near 48 and 46 K. The susceptibility at high temperature (not shown) is nearly isotropic and a fit of the $1/\chi$ data to a Curie-Weiss law furnishes effective

moments $\mu_{\text{eff}}=7.39$ and $7.52 \mu_B$ and paramagnetic Curie temperature $\theta_p = -11$ and -14 K for H along [001] and [100] respectively. These effective moments are lower than the free ion value of $7.94 \mu_B$ expected for Eu^{2+} ($g = 2$, $S = 7/2$), which is due either to the presence of residual In-flux or to a slight Eu off-stoichiometry, corresponding to about 10 at.% Eu deficit. As to polycrystalline EuIrSi_3 , its susceptibility is shown between 30 and 60 K in the inset of Fig.1: two anomalies (arrows) are also present, near 52 and 43 K, witnessing the same phenomenon as in EuRhSi_3 . The θ_p value is -17 K, while $\mu_{\text{eff}}=7.7 \mu_B$ is closer to the Eu^{2+} free ion value.

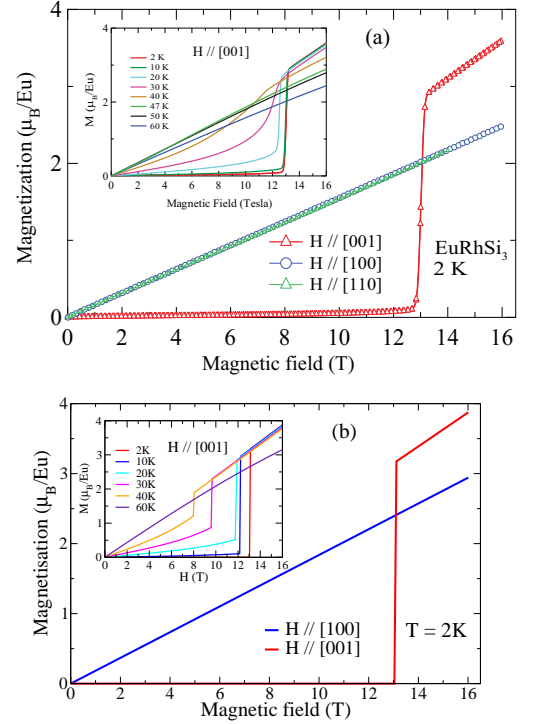


Fig. 2: (a) Isothermal magnetisation $M(H)$ of EuRhSi_3 at 2 K along major crystallographic directions. Inset: $M(H)$ curves at higher temperatures. (b) Simulation of the $M(H)$ curves in EuRhSi_3 according to the model described in the text. The calculated values are 10% higher than the data due to the assumed Eu mass deficit in the single crystal sample.

The Néel temperature in intermetallic compounds is the result of the indirect RKKY exchange between $4f$ spins \mathbf{S} mediated by the $4f$ -conduction electron coupling with constant J_{kf} :

$$\mathcal{H}_{kf} = -J_{kf} \mathbf{s} \cdot \mathbf{S}, \quad (1)$$

where \mathbf{s} is the conduction electron spin density, and it has the form: $T_N \propto J_{kf}^2 n(E_F) S(S+1)$ [1]. Its value in these materials, near 50 K, is much larger than in other members of the series (≈ 15 K), pointing to an enhanced value of $n(E_F)$.

The isothermal magnetisation versus field scan at 2 K in EuRhSi_3 , shown in Fig.2(a), is a textbook example of an antiferromagnet with the tetragonal [001] c -axis as

the easy axis of magnetisation and the (001) *ab*-plane as the hard plane, in line with the susceptibility data of Fig.1. For $H \parallel [001]$, an unusually large spin-flop field of 13 T is observed. A linear extension of the magnetisation curves for both field directions up to a saturation moment value $m_0 = 7 \mu_B$ yields large spin-flip fields $H_{sf}^c \simeq 28$ T and $H_{sf}^a \simeq 41$ T. The latter is larger since the field aligns the moments in the hard magnetic plane. In the standard molecular field theory [8], one has: $H_{sf}^c = 2(H_e - H_a)$ and $H_{sf}^a = 2(H_e + H_a)$, where H_e and H_a are respectively the exchange and the ‘‘anisotropy’’ field, the latter being defined as $H_a = K/m_0$ where K is the anisotropy energy density. Then we obtain $H_e = 17$ T and $H_a = 3.35$ T, and the critical spin-flop field $H_{cr} = 2\sqrt{H_a(H_e - H_a)} = 13.5$ T, in very good agreement with experiment. The spin-flop field in EuRhSi₃ is much larger than in EuNiGe₃ [6] (2-3 T), a logical consequence of a large H_e linked to the high T_N value.

In the inset of Fig.2(a) are plotted the magnetisation curves along the easy axis at higher temperature. On heating, the spin-flop field decreases and the jump at the spin-flop broadens.

Modeling. However, such a simple model as described above cannot account for the quite different values of T_N and $|\theta_p|$, and the oscillatory nature of the RKKY exchange compels one to introduce at least two different exchange integrals. Therefore, we use a numerical self-consistent calculation which has been described thoroughly in Ref. [6]: i) the infinite range dipolar interaction is added, ii) two exchange integrals J_1 (intra-plane first neighbor) and J_2 (interplane first neighbor) for the centered tetragonal structure are considered, as well as exchange anisotropy, and iii) the single ion crystalline anisotropy is described by a term DS_z^2 , where $Oz=c$. We also assume a magnetic structure made of ferromagnetic (*ab*) planes ($J_1 > 0$) coupled antiferromagnetically along *c* ($J_2 < 0$), i.e. a propagation vector $\mathbf{k}=[001]$. To obtain a first estimation of the exchange constants, the molecular field equations linking T_N and θ_p with J_a and J_c are used [5, 6], yielding: $J_a = 1.1$ K and $J_c = -0.88$ K. We have taken $T_N = 60$ K (see the section about Mössbauer spectroscopy) and a mean value $\theta_p = -13$ K. Figure 2(b) shows the curves which reproduce best the experimental data, with a small exchange anisotropy: $J_a^{\parallel} = 0.8$ K, $J_a^{\perp} = 1.1$ K, $J_c^{\parallel} = -0.7$ K, $J_c^{\perp} = -0.9$ K and a crystalline anisotropy parameter $D = -0.85$ K. The model yields $T_N = 57$ K and $\theta_p = -6$ and -17 K for $H \parallel [001]$ and $H \parallel [100]$ respectively (experimental values -11 and -14 K resp.). At 30 K and above, the model cannot exactly reproduce the smoothing of the spin-flop transition (see inset of Fig.2(b)).

Electrical resistivity. The electrical resistivity of EuIrSi₃ and EuRhSi₃ (and of non-magnetic LaIrSi₃) is shown in Figs.3(a) and (b). Above T_N it varies almost linearly up to 300 K in both compounds due to phonon scattering. It shows a small upturn at the magnetic transitions, likely caused by antiferromagnetic fluctuations just

above T_{N1} and decreases rapidly on cooling due to a strong depletion in the spin-disorder scattering in the magnetically ordered state. One striking feature is that the resistivity of polycrystalline EuIrSi₃ is one order of magnitude larger than that of single crystal EuRhSi₃. We reckon that this is probably due to strong grain boundary scattering which enhances the resistivity of the polycrystalline sample. The residual resistivity $\rho_0 = \rho(2\text{K})$ is lower than $10 \mu\text{Ohm.cm}$ in both materials (see Table 1), indicating they are chemically well ordered.

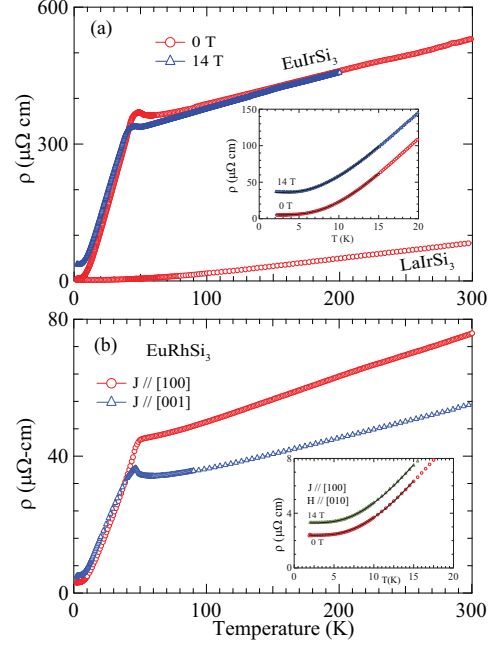


Fig. 3: (a) Electrical resistivity as a function of temperature $\rho(T)$ of EuIrSi₃ in zero field and in a 14 T field. (b) $\rho(T)$ data of EuRhSi₃ when current density $J \parallel [100]$ and $[001]$. The insets show the low temperature data together with their fit to Eq.(3).

The total spin disorder resistivity ρ_m , estimated as $\rho(T_N) - \rho_0$, amounts to about $35 \mu\text{Ohm.cm}$ in EuRhSi₃ while it is of the order of a few $\mu\text{Ohm.cm}$ in the other compounds of the series [2,3,6]. Since $\rho_m \propto J_{kf}^2 n(E_F) S(S+1)$ [1], its enhanced value in EuRhSi₃ is in line with a stronger $n(E_F)$.

In the AF phase below 20 K, magnon scattering is the dominant mechanism for resistivity. With an antiferromagnetic spin wave dispersion relation:

$$E(k) = \sqrt{\Delta^2 + \sigma k^2} \quad (2)$$

where Δ is the anisotropy gap and σ the spin-wave stiffness, the electrical resistivity in zero field for $T < \Delta$ is given by [9]:

$$\rho(T) = \rho_0 + A\Delta^2 \left(\frac{T}{\Delta}\right)^{1/2} e^{-\Delta/T} \times \left[1 + 2/3 \left(\frac{T}{\Delta}\right) + 2/15 \left(\frac{T}{\Delta}\right)^2 \right], \quad (3)$$

Table 1: Parameters obtained after fitting Eq.(3) to the zero field resistivity data of EuRhSi₃ with $J \parallel [001]$, and of EuIrSi₃.

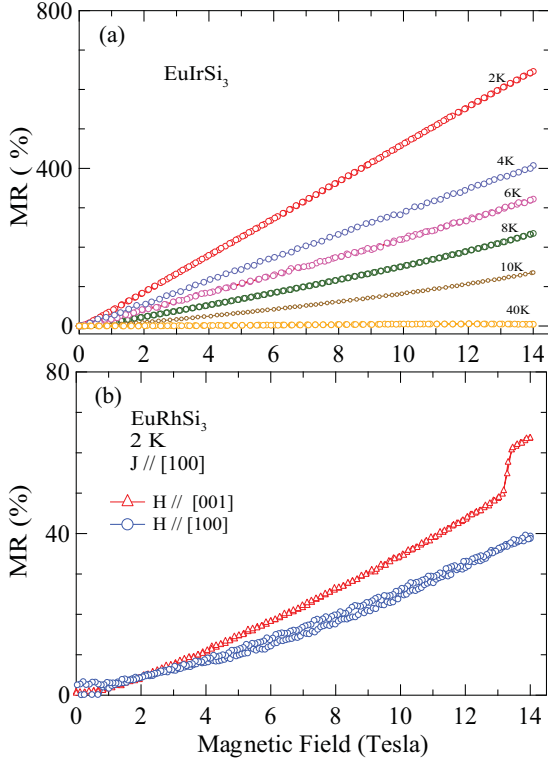
	$\rho_0(\mu\Omega \text{ cm})$	$A(\mu\Omega \text{ cm}/\text{K}^2)$	$\Delta(\text{K})$
EuRhSi ₃	5.1	0.04	23.3
EuIrSi ₃	5.27	0.43	25.2

where A a material dependent constant. Equation (3) provides a good fit to the zero field data in both compounds between 1.8 and 15 K (and also for a 14 T field), as shown by the solid lines in the insets of Fig.3. In EuIrSi₃, the zero field spin wave gap is 25.2 K and it is 23.5 K in EuRhSi₃. The AF spin wave gap is linked to the exchange and anisotropy fields H_e and H_a by the relation [10]:

$$\Delta = 2g\mu_B\sqrt{H_a(H_a + H_e)}. \quad (4)$$

Using the values determined above in EuRhSi₃: $H_e=17$ T, $H_a=3.35$ T and $g=2$, one obtains $\Delta = 22.1$ K, in excellent agreement with experiment in this material and close to the value in EuIrSi₃.

At a field of 14 T, ρ_0 increases to 35.9 $\mu\Omega\text{cm}$ in EuIrSi₃ and to 9 $\mu\Omega\text{cm}$ in EuRhSi₃ for $H \parallel [100]$ and $J \parallel [001]$.


Fig. 4: Magnetoresistance (MR) of EuIrSi₃ at different temperatures. (b) MR of EuRhSi₃ for $H \parallel [100]$ and $H \parallel [001]$ with $J \parallel [100]$ in both the cases.

The significant increase of ρ_0 with field corresponds to a positive magnetoresistance ratio MR , defined as $MR = [\rho(H) - \rho(H = 0)]/\rho(H = 0)$, as expected for anti-ferromagnets [11,12]. The plots of MR at selected temperatures in EuIrSi₃ are shown in Fig.4(a). It reaches giant

values: at 14 T, it exceeds 100% at 10 K and it reaches 600% at 2 K. At higher temperatures (not shown), MR decreases and becomes negative near 47 K, shows an absolute minimum near 50 K and has a small residual value of -3% at 200 K, far above T_{N1} . In EuRhSi₃, the MR is lower, as shown in Fig.4(b) at 2 K for $J \parallel [100]$ and $H \parallel [001]$ and $[100]$. A small positive jump in the MR occurs for $H \parallel [001]$ at the spin-flop field (13 T), although the MR is expected to drop to a small (positive) value above the spin-flop field, according to the molecular field calculation in Ref. [11].

Heat capacity. The main panels of Fig.5 show the heat capacity of EuIrSi₃ and EuRhSi₃ together with that of the non-magnetic La-reference. The two plots show two major peaks at 51.8 and 43.1 K in EuIrSi₃ and at 48.3 and 45.8 K in EuRhSi₃ in close correspondence with the anomalies seen in the susceptibility data, thus confirming the occurrence of two magnetic transitions in these two compounds. The jump in the heat capacity at the higher transition temperature T_{N1} is approximately 9.5 and 12 J/mol.K in the Ir and Rh-compound, respectively, which is lower than the value $\delta C_{7/2}=20.14$ J/mol.K for an equal moment anti-ferromagnetic transition for $S=7/2$ ions in the mean field model, and closer to that predicted for an amplitude modulated structure ($2/3 \delta C_{7/2}$) [2,13]. This suggests that at T_{N1} occurs a transition to a modulated moment structure. The transition from this intermediate structure to an equal moment structure takes place at T_{N2} . This behaviour is confirmed by the ¹⁵¹Eu Mössbauer spectra recorded at few selected temperatures.

Deep in the AF phase, the specific heat should be the sum of 3 terms [14]:

$$C(T) = \gamma T + \beta T^3 + B\Delta^4 \left(\frac{T}{\Delta}\right)^{1/2} e^{-\Delta/T} \quad (5)$$

$$\times \left[1 + 39/20 \left(\frac{T}{\Delta}\right) + 51/32 \left(\frac{T}{\Delta}\right)^2 \right],$$

where the first linear term is the conduction electron heat capacity, the second is the phonon contribution and the third the magnon heat capacity corresponding to a dispersion law given by Eq.(2) with a gap Δ . Equation (5) provides a good fit of the data between 1.8 and 10 K, shown by the solid line in the insets of Figs.5(a) and (b). For EuIrSi₃, the best fit estimates of γ and Δ are 30.5 mJ/mol.K² and 22.9 K respectively. The gap value is very close to that inferred from the resistivity data (25.2 K), which lends credibility to our analysis. In the case of EuRhSi₃, one obtains: $\gamma = 40.3$ mJ/mol.K² and $\Delta=17.6$ K, the latter value somewhat lower than the resistivity derived value (23.3 K). It may be noted that the Sommerfeld coefficient γ is an order of magnitude larger than in sp -metals, and even larger than in many d -metal alloys. The Sommerfeld coefficient is expressed as [10]: $\gamma = \frac{2}{3}\pi^2 k_B^2 n(E_F)$, and its large value must be related to an enhanced $n(E_F)$.

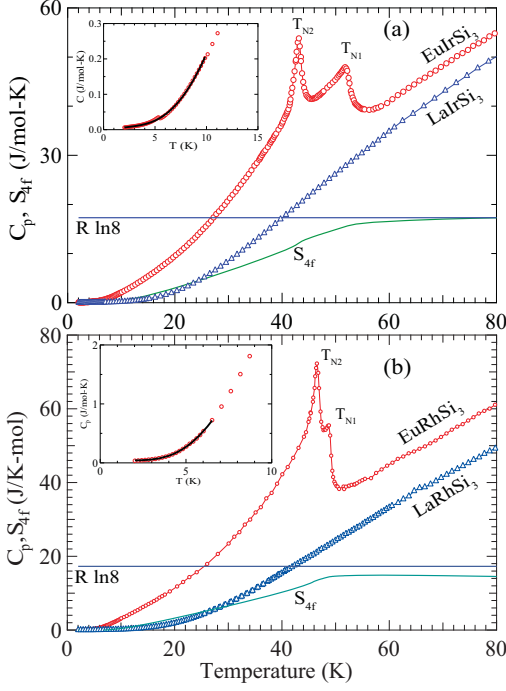


Fig. 5: (a) Variation of heat capacity with temperature $C(T)$ of EuIrSi₃ and of its non magnetic analogue LaIrSi₃. The solid green line represents the calculated entropy $S_{4f}(T)$. Inset shows the fitted Eq.(5) to the the low temperature data (b) $C(T)$ of EuRhSi₃ and LaRhSi₃ with a similar legend as for the upper panel.

The entropy S_{4f} associated with the magnetic ordering was estimated by integrating C_{4f}/T , where C_{4f} was obtained by subtraction from $C(T)$ of both the normalized heat capacity of LaT₃Si₃, taking into account the slight difference in the atomic masses of Eu and La, and the large conduction electron contribution γT . It is seen that S_{4f} attains the expected value of $R \ln 8$ (for $S = 7/2$ Eu²⁺ ions) close to T_{N1} in both compounds.

¹⁵¹Eu Mössbauer spectra. The Mössbauer spectra on the isotope ¹⁵¹Eu in EuIrSi₃ are shown in Fig.6 in the two temperature ranges defined as phase I ($T < 43.1$ K) and phase II (43.1 K $< T < 51.8$ K). Spectra in EuRhSi₃ are similar. The spectrum at 4.2 K is a standard hyperfine field pattern characteristic of Eu²⁺ ($S=7/2$, $L=0$), with an isomer shift relative to EuF₃ of $-7.92(5)$ mm/s which matches well with the value reported in Ref. [7]. This spectrum presents the peculiarity of a very high hyperfine field H_{hf} (4.2 K) = 52.6(3) T (51.6 T in EuRhSi₃). This high value can be explained by the large $n(E_F)$ prevailing in these materials. Indeed, in magnetically ordered intermetallic materials with the $L=0$ ion Eu²⁺, the hyperfine field is solely due to the spin polarisation of the s -type electrons at the nucleus site. It can be expressed as [15]: $H_{hf}(T) = A m(T) + H_{ce}$, where the first term is the core polarisation field proportional to the Eu²⁺ moment $m(T) = -g\mu_B \langle S \rangle_T$ and worth $\simeq 34$ T at saturation [16]. The second term H_{ce} is due to the conduction

electron spin polarisation $\langle s \rangle_T$ induced by the $4f$ shell through J_{kf} exchange and is given approximately by [15]: $H_{ce} \simeq A_{ce} \mu_B \langle s \rangle_T$, where A_{ce} is a hyperfine constant. According to Eqn.(1), the effective field on s is: $\frac{J_{kf} \mathbf{S}}{g\mu_B}$, and introducing the Pauli susceptibility: $\chi_P = 2 \mu_B^2 n(e_F)$, one obtains:

$$H_{ce} \simeq A_{ce} J_{kf} n(E_F) m(T). \quad (6)$$

In most Eu²⁺ intermetallic materials and in the other members of the series, the saturated hyperfine field amounts to about 30 T, i.e. H_{ce} is negative and worth a few T. In EuIrSi₃ and EuRhSi₃, due to the enhanced $n(E_F)$ value, H_{ce} is much larger ($\simeq 18$ T) and happens to be positive. The same situation holds in EuFe₄P₁₂, which presents the largest hyperfine field ever measured with ¹⁵¹Eu (67 T), implying $H_{ce} \simeq 33$ T [17].

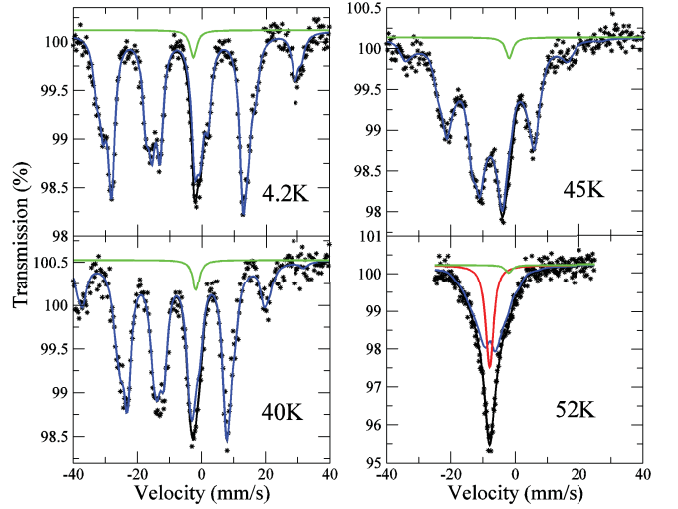


Fig. 6: ¹⁵¹Eu Mössbauer spectra in EuIrSi₃ at selected temperatures: in the commensurate phase (4.2 and 40 K), and in the incommensurate phase (45 and 52 K). The spectrum at 52 K is typical of the “coexistence” region, with a contribution from the paramagnetic phase of some part of the sample (red subspectrum) occurring in case of a first order transition. The green subspectrum represents an impurity phase containing Eu³⁺ (relative intensity 2%).

Whereas the spectra in phase I (below 43 K) show the presence of a unique hyperfine field, and hence of a unique Eu²⁺ magnetic moment, there occurs a sudden change of the spectral shape above 43 K, i.e. when entering phase II, where the spectra can be fitted to an incommensurate modulation of hyperfine fields [18]. The latter is well described by the first 3 odd harmonics of a Fourier series:

$$H_{hf}(kx) = h_1 \sin(kx) + h_3 \sin(3kx) + h_5 \sin(5kx) \quad (7)$$

where k is the propagation vector of the modulation and x the distance along k . The three coefficients h_1 , h_3 and h_5 were fitted to the spectral shape at each temperature to obtain the modulation profiles shown in Fig.7. The

modulation becomes more “squared” as temperature decreases and approaches the transition to the incommensurate phase.

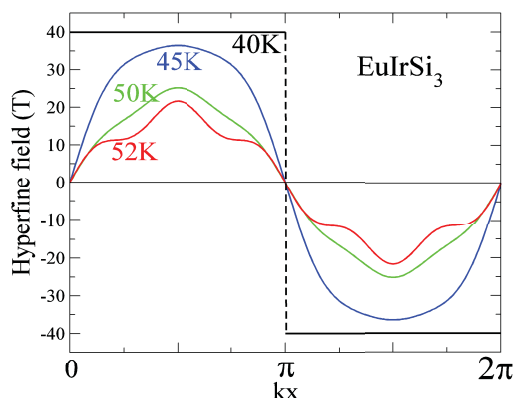


Fig. 7: Hyperfine field modulation over a period in EuIrSi_3 in the incommensurate modulated phase II at selected temperatures.

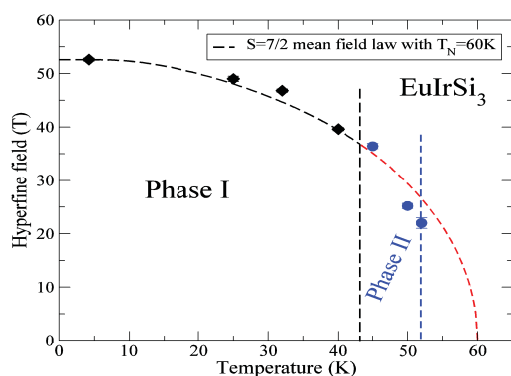


Fig. 8: In EuIrSi_3 , thermal variation of the hyperfine field in Phase I (black dots) and of the maximum of the hyperfine field modulation in Phase II (blue disks). The dashed line is the $S=7/2$ mean field law with $T_N=60\text{K}$, extrapolated in phase II above 43 K (in red).

The thermal variation of the hyperfine field is plotted in Fig.8. In phase I, the hyperfine field values approximately follow a mean field law for $S=7/2$, in line with its proportionality to the Eu^{2+} moment derived above. The transition temperature of this mean field law (60 K) does not correspond to the actual Néel temperature because of the presence of the commensurate - incommensurate transition at 43.1 K and of the first-order character of the transition to the paramagnetic phase at 51.8 K (see spectrum at 52 K in Fig.6).

Conclusion. –

The whole set of our thermodynamic and spectroscopic measurements in the two divalent Eu intermetallics EuIrSi_3 and EuRhSi_3 can be coherently and qualitatively interpreted by assuming a high density of electronic band states at the Fermi energy, which sets them apart from the other members of the EuTX_3 family. We attribute the

observed enhanced values to a large $n(E_F)$ rather than to an anomalously large $4f$ -conduction electron coupling J_{kf} since the Sommerfeld coefficient does not involve J_{kf} and there is *a priori* no reason for the stable Eu^{2+} $4f$ shell to be prone to strong hybridisation with the conduction band. The two compounds present a cascade of magnetic transitions near 50 K, from a paramagnetic to an incommensurate modulated, then to a commensurate antiferromagnetic phase. In the EuRhSi_3 single crystal sample, we could evidence an important anisotropy of the magnetisation, confirming the link between these two phenomena.

REFERENCES

- [1] SEE FOR INSTANCE FREEMAN A. J., *Magnetic properties of rare earth metals*, Chap.6, edited by ELLIOTT R. J., PLENUM PRESS, LONDON AND NEW YORK, 1972.
- [2] KUMAR N., DHAR S. K., THAMIZHAVEL A., BONVILLE P. and MANFRINETTI P., *Phys. Rev. B*, **81** (2010) 144414.
- [3] KUMAR N., DAS P. K., KULKARNI R., THAMIZHAVEL A., DHAR S. K. and BONVILLE P., *J. Phys.: Condens. Matter*, **24** (2012) 036005.
- [4] BEDNARCHUK O., GAGOR A. and KACZOROWSKI D., *J. Alloys Comp.*, **622** (2015) 432.
- [5] GOETSCH R. J., ANAND V. K. and JOHNSTON D. C., *Phys. Rev. B*, **87** (2013) 064406.
- [6] MAURYA A., BONVILLE P., THAMIZHAVEL A. and DHAR S. K., *J. Phys.: Condens. Matter*, **87** (2013) 064406.
- [7] CHEVALIER B., COEY J. M. D., LIORET B. and ETOURNEAU J., *J. Phys. C: Solid State Phys.*, **19** (1986) 4521.
- [8] HERPIN A., *Théorie du Magnétisme*, edited by PRESSES UNIVERSITAIRES DE FRANCE, PARIS, FRANCE(1968)
- [9] FONTES M. B., TROCHEZ J. C., GIORDANENGO B., BUD'KO S. L., SANCHEZ D. R., BAGGIO-SAITOVITCH E. M. and CONTINENTINO M. A., *Phys. Rev. B*, **60** (1999) 6781
- [10] KITTEL C., *Quantum theory of solids*, edited by JOHN WILEY AND SONS, NEW-YORK(1964)
- [11] YAMADA H. and TAKADA S., *Progr. Theor. Phys.*, **49** (1973) 1401
- [12] MCEWEN K. A., *Handbook on the Physics and Chemistry of rare Earths*, p.411, edited by GSCHNEIDER K. A. and EYRING L., NORTH-HOLLAND, AMSTERDAM,1978
- [13] BLANCO J. A., GIGNOUX D. and SCHMITT D., *Phys. Rev. B*, **43** (1991) 13145
- [14] CONTINENTINO M. A., DE MEDEIROS S. N., ORLANDO M. T. D., FONTES M. B. and BAGGIO-SAITOVITCH E. M., *Phys. Rev. B*, **64** (2001) 012404
- [15] BLEANEY B., *Magnetic properties of rare earth metals*, Chap.8, edited by ELLIOTT R. J., PLENUM PRESS, LONDON AND NEW YORK, 1972
- [16] NOWIK I., DUNLAP B. D. and WERNICK J. H., *Phys. Rev. B*, **8** (1973) 238
- [17] GÉRARD A., GRANDJEAN F., HODGES J. A., BRAUN D. J. and JEITSCHKO W., *J. Phys. C: Solid State Phys.*, **16** (1983) 2797
- [18] BONVILLE P., HODGES J. A., SHIRAKAWA M., KASAYA M. and SCHMITT D., *Eur. Phys. J. B*, **21** (2001) 349